

# Adsorption of Catechols, 2-Aminophenols, and 1,2-Phenylenediamines at the Metal (Hydr)Oxide/Water Interface: Effect of Ring Substituents on the Adsorption onto $TiO_2$

DHARNI VASUDEVAN<sup>†</sup> AND  
ALAN T. STONE\*

Department of Geography and Environmental Engineering,  
G. W. C. Whiting School of Engineering, The Johns Hopkins  
University, Baltimore, Maryland 21218

The extent of adsorption and the value of the adsorption equilibrium constant ( $K^s_{intr}$ ) for simple organic ligands is influenced by the identity of the ligand donor groups and other substituents on the aromatic ring. Catechols adsorb onto  $TiO_2$  to a significantly greater extent than 2-aminophenols; the adsorption of 1,2-phenylenediamines is negligible. The  $TiO_2$  surface has a high ionic contribution to bonding; ligands possessing donor groups with the highest ionic contribution to bonding adsorb to the greatest extent. A covalent contribution to bonding can increase binding to Ti(IV)-containing surfaces, but only when the ionic contribution is already strong. Within each ligand class, substituents alter the competition between protons and surface sites for binding the deprotonated ligand. For this reason,  $pK_{a1}$ ,  $pK_{a2}$ , and  $\log K^s_{intr}$  are all important in determining the extent of adsorption. Additionally, substituents that impart hydrophobicity also raise the extent of adsorption and the value of  $\log K^s_{intr}$ .

## Introduction

Organic ligands possess Lewis base functional groups (or ligand donor groups) containing oxygen, nitrogen, or sulfur atoms that are capable of forming bonds to protons, dissolved metal ions, and metal-containing mineral surfaces. The adsorption of organic ligands onto oxides, hydroxides, and other minerals is known to retard their migration in soils and aquifers and to alter their susceptibility toward chemical and biological transformations (1). The adsorption behavior of a number of organic ligands possessing carboxylic acid groups has been extensively

studied, and the effects of pH have been successfully modeled by choosing appropriate stoichiometries and equilibrium constants for adsorption (2–13). Less is known about the adsorption of organic compounds with hydroxyl or amino groups as the sole ligand donor group(s) (14–19).

This work is concerned with the adsorption of aromatic organic ligands possessing pairs of ligand donor groups (catechols, 2-aminophenols, and 1,2-phenylenediamines) onto titanium dioxide ( $TiO_2$ ). The objective is to evaluate how the structure of organic ligand pollutants determines the extent of adsorption onto metal (hydr)oxides. Our efforts have focused on understanding why the extent of adsorption and the value of the adsorption equilibrium constant ( $K^s_{intr}$ ) change when the identity of the ligand donor groups (hydroxyl vs amino) and other non-ligand substituents on the aromatic ring are varied. In addition, the effect of aqueous medium pH and ionic strength are investigated.

The above-mentioned classes of organic ligands were selected because they are important substructures of potentially toxic and carcinogenic pollutants from pharmaceutical, dyestuff, photographic, agrochemical, and metal plating industries. Adsorption behavior is examined with respect to one metal oxide ( $TiO_2$ ) in order to focus attention on the effect of ligand structure on adsorption behavior. Of the metal oxides encountered by organic pollutants in highly weathered soils (e.g., tropical soils),  $TiO_2$  is most resistant to dissolution. Therefore, it serves as a good model oxide to study adsorption behavior. Subsequent reports will describe adsorption onto oxides of iron and aluminum.

**Qualitative and Quantitative Approaches to Adsorption.** The adsorption of organic compounds represents the net balance of water–water, solute–solute, solute–surface, solute–water, and surface–water interaction forces. It is established that the partitioning of nonpolar hydrophobic organic compounds (HOCs) onto soil organic matter (20–23) is driven primarily by the hydrophobic effect (24); water–water interaction energies are lower than HOC–water interaction energies, resulting in HOC exclusion from bulk water (25, 26). Organic ligands differ from nonpolar HOCs in that they are polar and often ionizable. The interaction of an organic ligand ion with a charged surface adds an electrostatic component to the previously mentioned interaction forces. Additionally, the ligand donor atoms can induce a dipole moment and can facilitate hydrogen bonding. Thus, the degree of surface hydration (water–surface interaction forces), ligand–water interaction forces, and ligand–surface interaction forces all play a crucial role in determining the extent of organic ligand adsorption. These interaction forces are interrelated and therefore difficult to quantify individually.

In view of this, previous studies of ligand adsorption have classified interactions at the metal (hydr)oxide–water interface into two categories: (i) those arising from long-range electrostatic forces and (ii) all other interactions that are difficult to quantify individually are collectively referred to as near-range physical and chemical forces (15).

Long-range electrostatic forces affecting the distribution of ions near charged surfaces can be estimated from surface charge, solution species charge, and ionic strength of the

\* Corresponding author fax: 410-516-8996; e-mail address: DOG\_ZATS@JHUVMS.HCF.JHU.EDU.

<sup>†</sup> Present address: American Chemical Society, Government Relations and Science Policy, Washington, DC.

TABLE 1

## Properties of Ligands Included in This Study

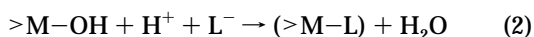
name	substituent	$\sigma_p$	$pK_{a1}$ (measd)	$pK_{a2}$ (measd)	$pK_{a1}^e$ (est)	$pK_{a2}^e$ (est)	$\log K_{ow}$	$\log S_m^h$ (mol/L)	$\log K_{intr}^s$
4-methyl-2-aminophenol	CH <sub>3</sub>	-0.14 <sup>a</sup>	4.3 <sup>d</sup>	10.0 <sup>d</sup>	4.99	10.21	1.11 <sup>f</sup>	-1.420	12.23
2-aminophenol	H	0.0 <sup>a</sup>	4.7 <sup>c</sup>	9.9 <sup>c</sup>			0.62 <sup>f</sup>	-1.33	12.07
4-phenyl-2-aminophenol	C <sub>6</sub> H <sub>5</sub>	0.05	4.4 <sup>d</sup>	9.7 <sup>d</sup>	4.68	9.78	2.51 <sup>g</sup>	-3.50	12.68
3-amino-2-naphthol	na	0.11 <sup>b</sup>	3.9 <sup>d</sup>	9.2 <sup>d</sup>	4.15	9.66	1.79 <sup>g</sup>	-3.04	11.92
4-chloro-2-aminophenol	Cl	0.24 <sup>a</sup>	3.9 <sup>d</sup>	9.3 <sup>d</sup>	3.78	9.36	1.81 <sup>f</sup>	-2.07	11.51
4-nitro-2-aminophenol	NO <sub>2</sub>	0.81 <sup>a</sup>	3.1 <sup>d</sup>	7.6 <sup>d</sup>	2.83	8.0	1.53 <sup>f</sup>	-1.57	10.89
2,3-dihydroxynaphthalene	na	0.11 <sup>b</sup>	8.89 <sup>c</sup>	12.93 <sup>c</sup>			2.05 <sup>g</sup>	-2.63	21.81
4-chlorocatechol	Cl	0.24 <sup>a</sup>	8.77 <sup>c</sup>	12.73 <sup>c</sup>			1.98 <sup>g</sup>	-2.32	20.52
4-nitrocatechol	NO <sub>2</sub>	0.81 <sup>a</sup>	6.88 <sup>c</sup>	11.24 <sup>c</sup>			1.66	-2.36	18.38
2,3-diaminonaphthalene	na	na	<1 <sup>d</sup>	4.1 <sup>d</sup>	0.89	4.35	0.86 <sup>g</sup>	-1.78	
4-chloro-1,2-phenylenediamine	Cl	0.24 <sup>a</sup>	<1 <sup>d</sup>	3.9 <sup>d</sup>	0.074	3.53	1.28 <sup>f</sup>	-0.14	
4-nitro-1,2-phenylenediamine	NO <sub>2</sub>	0.81 <sup>a</sup>	<1 <sup>d</sup>	2.7 <sup>d</sup>	-0.18	2.57	0.88 <sup>f</sup>	-1.83	

<sup>a</sup> Values cited in March (48). <sup>b</sup>  $\sigma$  value for annelated benzene ring in 2-naphthol cited in Barlin and Perrin (38). <sup>c</sup> Literature values cited in Martell and Smith (56). <sup>d</sup> Values measured by procedure outlined in the Materials and Methods section of text. <sup>e</sup> Estimated using linear free energy relationships reported by Barlin and Perrin (38) and Clark and Perrin (39) (estimates not made if literature values were available). <sup>f</sup> Measured values of  $\log K_{ow}$  (octanol-water partition coefficient) reported in the computer program ClogP (40). <sup>g</sup>  $\log K_{ow}$  calculated using ClogP. <sup>h</sup>  $\log S_m$  (aqueous solubility) calculated from a semi-empirical relationship developed by Yalkowsky and Valvani (47).

aqueous medium. According to the Gouy-Chapman theory of a single flat double layer (27), the activity of ions at the plane of closest approach ( $\{i\}_o$ ) is related to the activity of ions in bulk solution ( $\{i\}_b$ ) as follows:

$$\{i\}_o = \{i\}_b \exp(-z_i F \psi_o / RT) \quad (1)$$

where  $z_i$  is the charge on species  $i$ ,  $F$  is the Faraday constant,  $\psi_o$  is the electrical potential at the plane of closest approach (o),  $R$  is the gas constant, and  $T$  is the temperature. By accounting for electrostatic interactions using eq 1, the concentration at the plane of closest approach ( $\{i\}_o$ ) can be calculated from experimentally determined values of bulk concentrations ( $\{i\}_b$ ). An intrinsic adsorption equilibrium constant ( $K_{intr}^s$ ) for a particular adsorption stoichiometry can then be defined based upon the activity of the species at the plane of closest approach. An illustration is provided below:



$$K_{intr}^s = \frac{\{>M-L\}}{\{>M-OH\}\{L^-\}_o\{H^+\}_o} \quad (3)$$

$K_{intr}^s$  as defined in eq 3 incorporates the long-range electrostatic interactions and represents the cumulative effect of all of the near-range physical and chemical forces.

As evident from the previous discussion, a value for  $K_{intr}^s$  that is independent of pH and oxide loading (g of TiO<sub>2</sub>/L of solution) can be determined from experimental data by invoking mass balance, equilibrium relationships, equations that account for long-range electrostatic interactions, and fitted values for the adsorption stoichiometry. This exercise can be successfully performed using one of a number of available computer programs (28-31).

Most equilibrium computer models represent neutral surface sites as  $>M-OH^o$  since the exact coordinative structure of neutral sites is unknown. Spectroscopic studies have shown the existence of surface-bound metal ions with one, two, or more coordination positions exposed to the surrounding aqueous phase (edge, kink, adatom, and ledge sites) (32). In the absence of other adsorbates, both hydroxide ions and water molecules are coordinated to these surface sites (33, 34).

From the point of view of inner-sphere ligand adsorption, the representation of the neutral surface site as  $>M-OH$  merits reexamination. This representation may be misleading because it excludes the coordination of water molecules to surface metal ions and assumes that only one OH<sup>-</sup> ion is coordinated to the surface metal. Furthermore, this representation implies that inner-sphere adsorption of a monodentate ligand displaces the surface-bound OH<sup>-</sup> ion, thereby increasing the protonation level by one unit (displacement of a coordinated OH<sup>-</sup> ion is equivalent to gaining one H<sup>+</sup>). There is, however, no reason to dismiss the possibility that a surface-bound H<sub>2</sub>O molecule is displaced during adsorption, leaving the protonation level unaltered.

Bidentate ligands occupying two coordinative positions only confound the problem. In principle, the datum surface site can be represented in three ways. Writing the site as  $>M-(OH)_2$  requires the displacement of two OH<sup>-</sup> ions, increasing the protonation level by two units;  $>M-(OH)(H_2O)$  requires the displacement of one OH<sup>-</sup> ion and one H<sub>2</sub>O molecule, increasing the protonation level by one unit;  $>M-(H_2O)_2$  requires the displacement of two H<sub>2</sub>O molecules, leaving the protonation level unaltered. Alternative representations for surface-sites varying in the number of surface bound OH<sup>-</sup> ions and H<sub>2</sub>O molecules have also been proposed (5, 14, 35-37). Implicit in all of these representations is a predisposition concerning changes in protonation level. The accuracy of these representations will ultimately be tested by spectroscopic techniques.

## Materials and Methods

All solutions and suspensions were prepared from distilled, deionized water (DDW, Millipore Corp.). The glassware was soaked in 5 N nitric acid and rinsed several times with DDW before use. 4-Phenyl-2-aminophenol, 4-chlorocatechol, and 4-chloro-1,2-phenylenediamine were purchased from Tokyo Kasei (98+% purity). All other compounds were purchased from Aldrich Chemical Co. (96% purity and greater). HPLC-grade organic solvents were purchased from Baker.

Pertinent organic ligand properties are listed in Table 1, and structures are shown in Figure 1. The  $pK_a$  values of some of the test compounds were determined in our

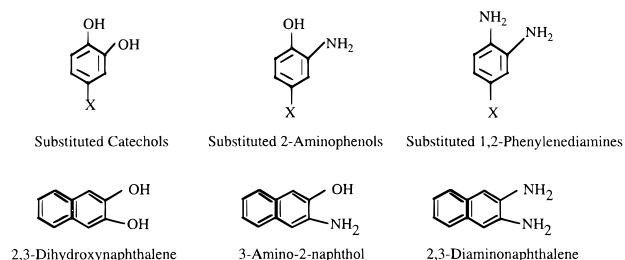


FIGURE 1. Structures of the ligands included in this study.

laboratory using UV spectrophotometry (Shimadzu UV-160). A low concentration of the test compound ( $5 \times 10^{-5}$  M) was titrated with HCl or NaOH. An ionic strength modifier was not added; the ionic strength of the medium was calculated to be close to  $1 \times 10^{-3}$  M. Absorbance was measured at two or three selected wavelengths as a function of pH. The inflection points in the plot of absorbance as a function of pH corresponds to the  $pK_a$ . The  $pK_a$  values were also estimated from compound structure using established linear free energy relationships (38, 39). Estimated and measured values agree within 0.5 log unit. The estimated  $pK_{a1}$  value for the 4-methyl-2-aminophenol is an exception; the calculated value is 0.69 log unit greater than the measured value. Octanol-water partition coefficients ( $\log K_{ow}$ ) for the test compounds were determined using the computer program ClogP (40). This program calculates  $\log K_{ow}$  from compound structure and compares predicted values with experimental values (where available). For each test ligand, the aqueous solubility ( $S_m$ ) (in mol/L) was estimated from a semi-empirical relationship developed by Yalkowsky and Valvani (41).

TiO<sub>2</sub> (type P25) was obtained from Degussa Corporation. Results from transmission electron microscopy and electron diffraction studies indicated that the TiO<sub>2</sub> sample was either anatase or brookite. The BET surface area, measured using N<sub>2</sub> adsorption, was found to be 39.5 m<sup>2</sup>/g (Micromeritics Flowsorb II 2300). The surface site density (total number of surface sites/nm<sup>2</sup> of surface) of the TiO<sub>2</sub> surface can be estimated in a number of ways including F<sup>-</sup> adsorption (42). A F<sup>-</sup> adsorption isotherm was conducted at pH 4.0 and yielded an adsorption maximum of  $2.5 \times 10^{-4}$  mol of F<sup>-</sup>/g of TiO<sub>2</sub>. Using the BET surface area quoted earlier, the surface site density was calculated to be between 3 and 4 sites/nm<sup>2</sup>.

Acid/base titrations of TiO<sub>2</sub> were performed in our laboratory at three different ionic strengths by Torrents (43). From the calculations of surface charge as a function of pH, it was determined that the  $pH_{zpc}$  for this material is 6.3. The following surface protonation constants were determined at an ionic strength of 0.1 M using the extrapolation to zero surface charge technique discussed by Stumm and Morgan (27):  $K_{a1}^s = 10^{-3.9}$  and  $K_{a2}^s = 10^{-8.7}$  (43). An earlier study by Berube and deBruyn (44) reported surface  $pK_a$  values for anatase also determined at 0.1 M ionic strength. The  $pK_a$  values determined by these two studies are in agreement.

**Adsorption Experiments.** Predetermined amounts of TiO<sub>2</sub> and DDW were added to 25-mL amber vials, sealed with Teflon septa, and allowed to equilibrate for a minimum of 30 min. The suspensions were then spiked with the test compound, and the pH was set by the addition of HCl or NaOH. Suspensions were continuously stirred with Teflon-covered magnetic stir bars throughout the experiment. After allowing for the required contact time for adsorption, an

aliquot of the suspension was removed and centrifuged (Eppendorf 5415 Microcentrifuge, at 13000 rpm for 15 min).

The concentration of organic ligand present in the supernatant solution was determined by HPLC (Waters Corp.) using a multiple-wavelength UV detector and a  $3.9 \times 300$  mm  $\mu$ Bondapak-C<sub>18</sub> column (Waters Corp.). The mobile phase employed for the analysis of NH<sub>2</sub>-containing ligands was a mixture of 50 parts methanol and 50 parts pH 6.5 aqueous solution of Na<sub>2</sub>HPO<sub>4</sub>/NaH<sub>2</sub>PO<sub>4</sub> ( $5 \times 10^{-2}$  M), triethylamine ( $1 \times 10^{-2}$  M), and acetate ( $1 \times 10^{-2}$  M). A mixture of 40 parts acetonitrile and 60 parts pH 3.5 aqueous solution of H<sub>3</sub>PO<sub>4</sub> ( $1 \times 10^{-3}$  M), triethylamine ( $1.25 \times 10^{-2}$  M), and acetate ( $1.25 \times 10^{-2}$  M) was used for the analysis of the substituted catechols and 2,3-dihydroxynaphthalene. The extent of adsorption was calculated from mass balance; the concentration present in the supernatant was subtracted from the total ligand concentration to obtain the concentration adsorbed.

The following experiments were conducted for each of the organic ligands examined in this study:

**Compound Stability.** The stability of the test ligand was assessed by monitoring the concentration of the compound in TiO<sub>2</sub>-free solution as a function of time and pH. For those compounds susceptible to oxidation, adsorption experiments were conducted in an anaerobic glove bag.

**Kinetic Study.** In order to determine the contact time required for adsorption, the extent of adsorption was measured as a function of time for 24–36 h. For all the compounds included in this study, the extent of adsorption reached a constant value after 15–30 min (with the exception of 4-phenyl-2-aminophenol, which required 24 h). For all subsequent experiments, at least 30 min was allowed for adsorption to take place.

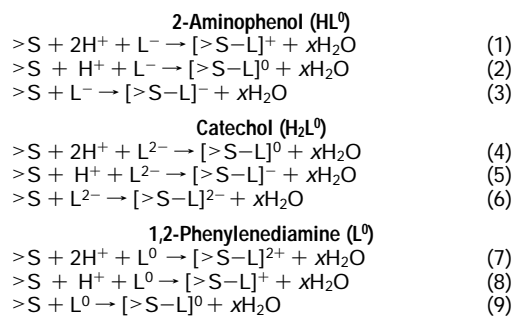
**Effect of Total Ligand Concentration.** Adsorption was measured at different total ligand concentrations (from  $1 \times 10^{-5}$  to  $5 \times 10^{-3}$  M) at a fixed pH and oxide loading. For oxide loadings in the range of 0.5–15 g/L, it was found that a total ligand concentration of  $5 \times 10^{-5}$  M fulfills four objectives: (i) it falls within the linear range of the concentration isotherm, (ii) it is the lowest concentration that allows measurements of adsorption as high as 90% by HPLC analysis, (iii) it is below the solubility of the test compounds, and (iv) it results in surface coverage that is not high enough to significantly alter surface charge. For these reasons, a total ligand concentration of  $5 \times 10^{-5}$  M was selected for all subsequent experiments.

**Effect of pH.** Experiments were performed to measure the extent of adsorption as a function of pH (in the pH range 2–11) at a fixed oxide loading and total ligand concentration. The pH was set by the addition of HCl or NaOH. The pH dependence was examined at low ionic strength (no electrolyte added) and at high ionic strength (0.1 M NaCl).

**Effect of Oxide Loading.** Consider a series of adsorption experiments performed at fixed system conditions with a set of ligands possessing different values of  $K_{intr}^s$ . When  $K_{intr}^s$  values are high enough that nearly 100% adsorption is attained, the predicted extent of adsorption is insensitive to further increases in the value  $K_{intr}^s$ . Likewise, when  $K_{intr}^s$  values are so low that it becomes difficult to distinguish the existence of adsorption from its absence, the predicted extent of adsorption is insensitive to further decreases in the value of  $K_{intr}^s$ . Because of these considerations, along with the precision and accuracy of our analytical methods,  $K_{intr}^s$  values can only be reliably measured from experiments

TABLE 2

## Possible Reaction Stoichiometries for Adsorption of Catechols, 2-Aminophenols, 1,2-Phenylenediamines, and Structurally Related Compounds



where the maximum extent of adsorption is greater than 5% and less than 95%. To meet this criterion, oxide loadings were systematically varied at a fixed total ligand concentration ( $5 \times 10^{-5}$  M) until the maximum extent of adsorption fell within the desired range.

**Desorption Study.** Attempts were made to recover the adsorbed organic ligand to ensure that loss from solution was due to adsorption and not degradation. In order to bring about desorption, the suspension pH was lowered to 2 by the addition of 1 M HCl, and sufficient NaF was added to yield a suspension concentration of  $5 \times 10^{-3}$  M. For most of the compounds examined, about 90–95% of the total ligand concentration was recovered. 2,3-Dihydroxynaphthalene was the exception; only 80–85% was recovered.

**Modeling.** The adsorption equilibrium constant ( $K_{intr}^s$ ) and the adsorption stoichiometry were determined using the computer program FITEQL 3.1 (28). This program determines equilibrium constants from experimental data using an optimization procedure. The diffuse layer model was used because it provides a representation of ligand adsorption at fixed ionic strength using the smallest number of fitting parameters. All the surface sites were assumed to be chemically identical.

For the equilibrium problem posed, FITEQL requires the input of both oxide surface attributes (oxide loading in g/L, oxide surface area in m<sup>2</sup>/g, surface site concentration in mole sites/L of suspension, and protonation constants,  $K_{a1}^s$  and  $K_{a2}^s$ ) and test ligand attributes (protonation constants,  $K_{a1}$  and  $K_{a2}$ ). The electrolyte concentration and ion charge are also required. Three different adsorption stoichiometries were examined for all ligands (Table 2). Each adsorption reaction is written in terms of the hypothetical neutral surface site and the fully deprotonated form of each ligand and postulates a stated change in surface protonation level and surface charge as organic ligand adsorption takes place. Since the exact coordinative structure of the neutral surface site is currently unknown, we would like to use a representation that has no bias concerning changes in protonation level during ligand adsorption. For this reason, no assumptions are made regarding the number of OH groups and water molecules bound to the surface metal ion, and the datum surface sites are simply represented as  $>S$  (Table 2). The charge on the surface is dealt with in the conventional manner; the neutral surface site is the datum, protonation yields a positively charged site, and deprotonation yields a negatively charged site.

The FITEQL optimization procedure was employed using each one of the three adsorption stoichiometries (Table 2). The adsorption stoichiometry that yields a pH dependence that most closely matches adsorption data (the best fit adsorption stoichiometry) was identified, and the value of  $K_{intr}^s$  corresponding to the best fit adsorption stoichiometry was reported. For the optimization procedure calculating  $K_{intr}^s$ , an experimental error of  $\pm 0.01$  was allowed for the pH values and an error of  $\pm 1 \times 10^{-6}$  M was allowed for the value of the adsorbed ligand concentration. The modeling exercises were constrained to use only one stoichiometry for adsorption and one fitting parameter,  $\log K_{intr}^s$ . These constraints facilitate ligand-to-ligand comparison of  $\log K_{intr}^s$  values. Values of  $\log K_{intr}^s$  were determined from experiments with a total ligand concentration of  $5 \times 10^{-5}$  M, an ionic strength of 0.1 M, and a TiO<sub>2</sub> loading of 1 g/L (for substituted catechols and 2,3-dihydroxynaphthalene) or 10 g/L (for substituted 2-aminophenols and 3-amino-2-naphthol).

For each test ligand examined, experiments were conducted to determine the extent of adsorption as a function of pH and ionic strength. The adsorption stoichiometry and the value of  $K_{intr}^s$  were then determined using the 0.10 M ionic strength experimental data and the diffuse layer model. Finally, the resulting differences in the extent of adsorption and the value of  $K_{intr}^s$  were used to interpret the physical and chemical phenomena governing adsorption.

## Results

All organic compounds included in this study possess two Lewis base groups. Preliminary experiments indicated that 2-aminophenol adsorbs to a significant extent, while 3-aminophenol and 4-aminophenol do not (15). Similarly, catechols adsorb to a significant extent onto TiO<sub>2</sub>, while hydroquinone adsorption is negligible. It can be concluded that the positioning of the two Lewis base groups (OH and/or NH<sub>2</sub>) ortho to one another is usually necessary for significant adsorption to occur. (2,4-Dinitrophenol and other very acidic phenols are important exceptions; see ref 15.)

**Adsorption Behavior of 2-Aminophenols.** 4-Nitro-2-aminophenol adsorbs more strongly onto TiO<sub>2</sub> than the other substituted 2-aminophenols examined. The filled symbols in Figure 2A illustrate that 4-nitro-2-aminophenol adsorption increases with increasing pH until a plateau is attained. The plateau of maximum adsorption lies between  $pK_{a1}$  and  $pK_{a2}$ ; increasing the pH above  $pK_{a2}$  causes adsorption to diminish to negligible levels. Model fits shown in Figure 2A correspond to each of the three alternative stoichiometries for adsorption listed in Table 2. Equation 2 (Table 2) provides the best fit: a neutral surface site along with a H<sup>+</sup> ion and a 4-nitro-2-aminophenolate anion (L<sup>-</sup>) react to form a surface complex with no net charge. Equation 1, yielding a positively charged surface complex, and eq 3, yielding a negatively charged surface complex, provide poor fits to the experimental data.

Figure 3A depicts adsorption behavior as a function of pH and oxide loading. The height and width of the plateau of maximum adsorption increases as the loading is increased. Modeling results indicate that  $K_{intr}^s$  determined at an oxide loading of 10 g/L can predict adsorption behavior at other loadings. Figure 4A shows that a change in ionic strength from  $1 \times 10^{-3}$  to 0.1 M does not significantly affect the experimentally measured extent of adsorption. Model

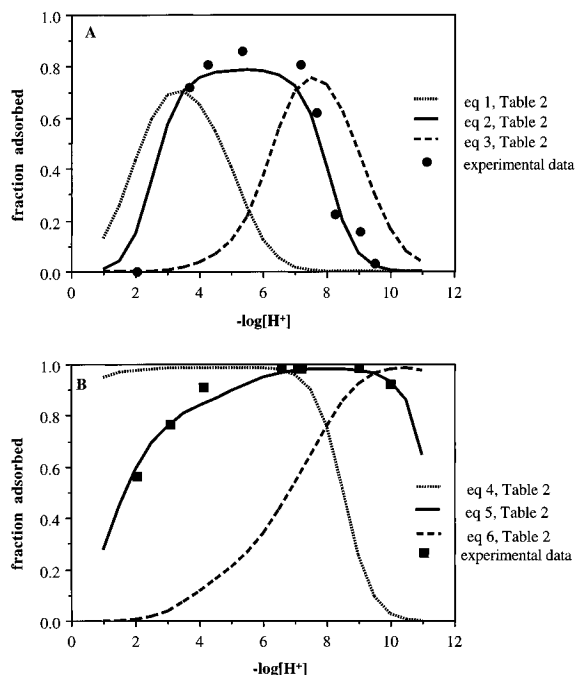


FIGURE 2. Diffuse layer model results based on adsorption stoichiometries listed in Table 2: (A)  $5.02 \times 10^{-5}$  M 4-nitro-2-aminophenol, 10 g/L  $TiO_2$ , and 0.1 M NaCl; (B)  $4.87 \times 10^{-5}$  M 4-nitrocatechol, 1 g/L  $TiO_2$ , and 0.1 M NaCl. The symbols represent experimental data, and the lines represent model results.

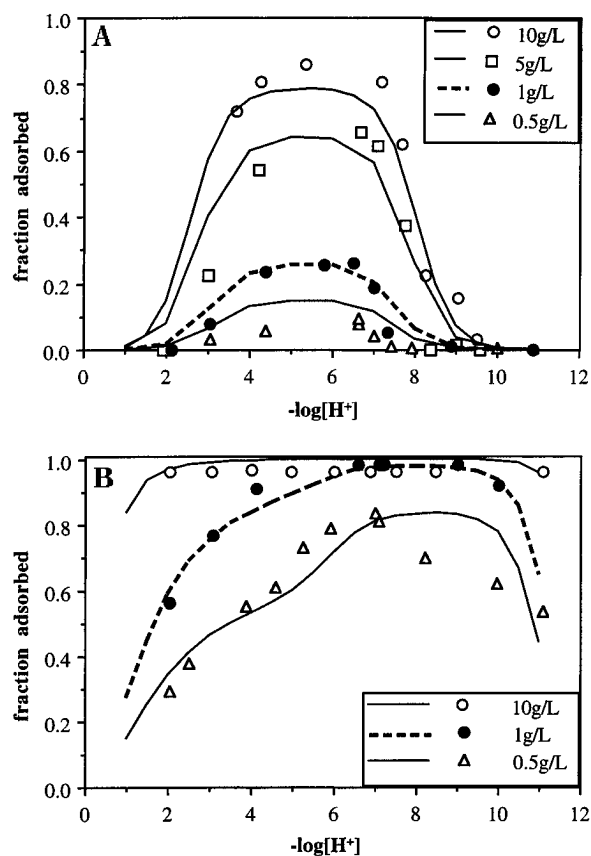


FIGURE 3. Adsorption of  $5 \times 10^{-5}$  M (A) 4-nitro-2-aminophenol and (B) 4-nitrocatechol as a function of pH and oxide loading (0.1 M NaCl). The symbols represent experimental data, and the lines represent model results.

results show that  $K_{intr}^s$  determined from experiments conducted at an ionic strength of 0.1 M (NaCl) can

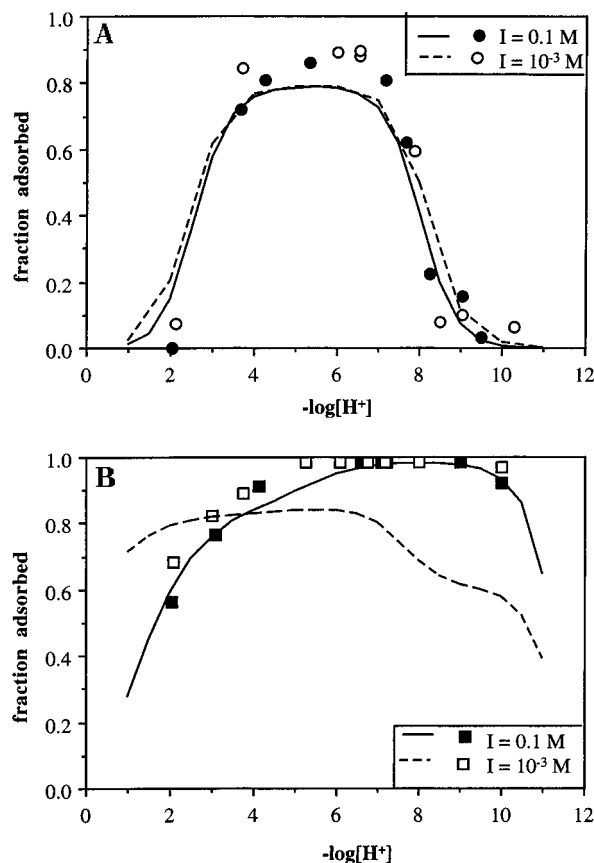


FIGURE 4. Effect of ionic strength on the adsorption behavior of (A)  $5.02 \times 10^{-5}$  M 4-nitro-2-aminophenol and 10 g/L  $TiO_2$ ; (B)  $4.87 \times 10^{-5}$  M 4-nitrocatechol and 1 g/L  $TiO_2$ . The symbols represent experimental data, and the lines represent model results.

successfully predict adsorption behavior at a lower ionic strength.

The adsorption behavior of five substituted 2-aminophenols and the structurally related compound 3-amino-2-naphthol was examined to explore the effect of ring substituents on the extent of adsorption and the value of  $\log K_{intr}^s$ . Experimental measurements and model results are shown in Figure 5A–C. As is the case with 4-nitro-2-aminophenol, the placement and the width of the plateau of maximum adsorption are set by  $pK_{a1}$  and  $pK_{a2}$ . The plateau becomes shifted toward more acidic pH values for 4-nitro-2-aminophenol (Figure 5A) because its  $pK_{a1}$  and  $pK_{a2}$  values are significantly lower than are those of the other ligands (Table 1). As with 4-nitro-2-aminophenol, the experimentally measured adsorption for the other substituted 2-aminophenols and 3-amino-2-naphthol are also best fit by the adsorption stoichiometry represented by eq 2 (Table 2). The values of  $\log K_{intr}^s$  determined from the best fit at a  $TiO_2$  loading of 10 g/L (Figure 5A–C) are listed in Table 1.

Table 1 indicates that the substituted 2-aminophenols differ in basicity (reflected by  $pK_{a1}$  and  $pK_{a2}$ ) and solvation properties (reflected by  $K_{ow}$  and  $S_m$ ). 4-Nitro-2-aminophenol adsorbs to the greatest extent despite possessing the lowest  $pK_a$  value. The  $pK_a$  values of the other five ligands are comparable. Of these five ligands, the height of the plateau of maximum adsorption for 2-aminophenol, 4-methyl-2-aminophenol, and 4-chloro-2-aminophenol is similar, while the height of the plateau for 4-phenyl-2-aminophenol and 3-amino-2-naphthol is significantly greater. Both 4-phenyl-2-aminophenol and 3-amino-2-

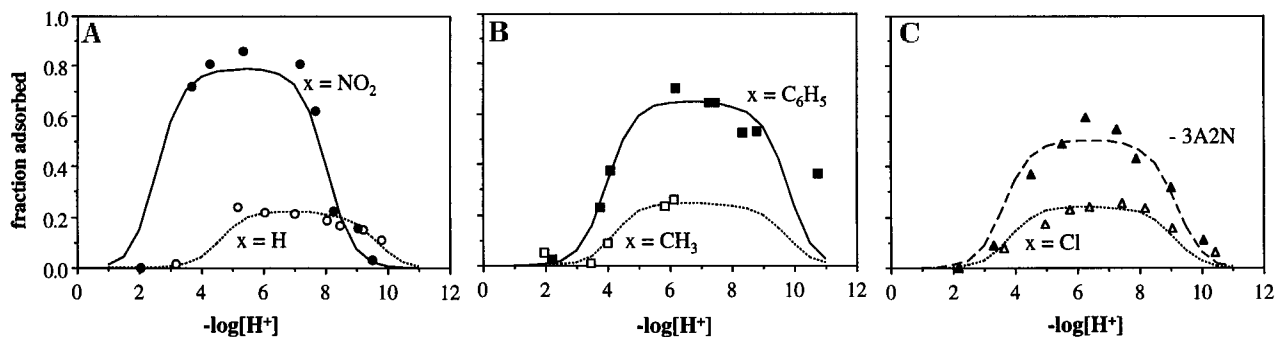


FIGURE 5. Adsorption of  $5 \times 10^{-5}$  M substituted 2-aminophenols and 3-amino-2-naphthol (3A2N) as a function of pH in suspensions containing 10 g/L  $\text{TiO}_2$  and 0.1 M NaCl. The symbols represent experimental data, and the lines represent model fits used to determine  $K^{\text{S}}_{\text{intr}}$ .

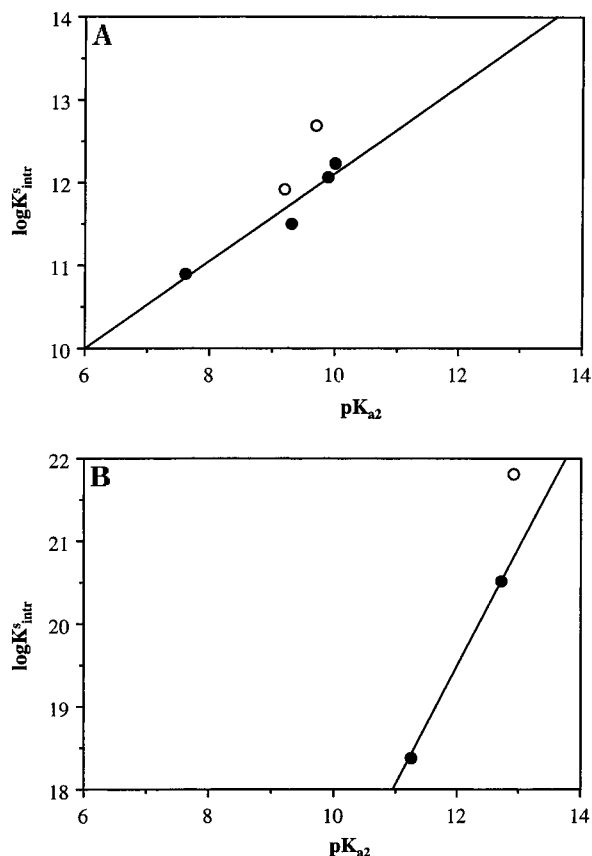


FIGURE 6.  $\log K^{\text{S}}_{\text{intr}}$  as a function of  $\text{p}K_{\text{a}2}$  for (A) substituted 2-aminophenols and 3-amino-2-naphthol and (B) substituted catechols and 2,3-dihydroxybenzene. Compounds with an additional aromatic ring (open symbols) are omitted from the correlation. For both ligand classes, a correlation between  $\text{p}K_{\text{a}1}$  and  $\log K^{\text{S}}_{\text{intr}}$  showed the same trend.

naphthol differ from the other ligands in that they possess an additional aromatic ring as a part of their compound structure and possess higher  $K_{\text{ow}}$  values and lower  $S_{\text{m}}$  values. Figure 6A shows that  $\log K^{\text{S}}_{\text{intr}}$  values generally increase as compound  $\text{p}K_{\text{a}}$  values increase. Those ligands with an additional aromatic ring, 4-phenyl-2-aminophenol and 3-amino-2-naphthol, fall above the line that correlates  $\log K^{\text{S}}_{\text{intr}}$  with  $\text{p}K_{\text{a}1}$  and  $\text{p}K_{\text{a}2}$ . It is important to note that 4-nitro-2-aminophenol, adsorbs to the greatest extent despite possessing the lowest  $\text{p}K_{\text{a}}$  values and the lowest  $\log K^{\text{S}}_{\text{intr}}$ .

**Adsorption Behavior of Catechols.** The adsorption behavior of 2-aminophenols is compared to that of catechols in order to determine how the identity of the Lewis base groups affects adsorption. At an oxide loading of 1 g/L (illustrated by the bold dashed lines and the filled circles,

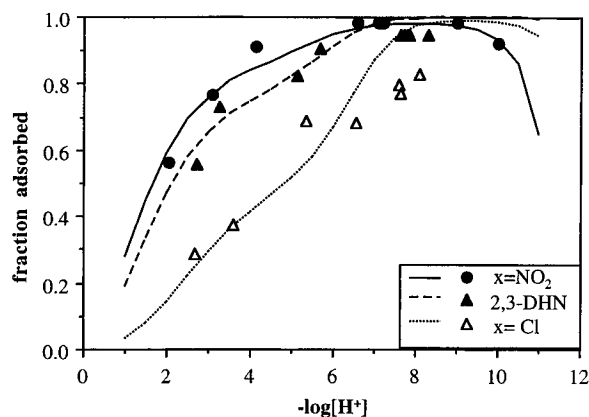


FIGURE 7. Adsorption of  $5 \times 10^{-5}$  M 4-nitrocatechol, 4-chlorocatechol, and 2,3-dihydroxynaphthalene (2,3-DHN) as a function of pH in suspensions containing 1 g/L  $\text{TiO}_2$  and 0.1 M NaCl. The symbols represent experimental data, and the lines represent model fits used to determine  $K^{\text{S}}_{\text{intr}}$ .

Figure 3A,B) 4-nitrocatechol adsorbs to a significantly greater extent than 4-nitro-2-aminophenol over the entire pH range. This same observation is also borne out at oxide loadings of 0.5 and 10 g/L.

Several similarities exist between the adsorption behavior of catechols and 2-aminophenols: (i) adsorption increases with pH, reaches a plateau in the pH range between the two  $\text{p}K_{\text{a}}$  values, and decreases at pH values greater than  $\text{p}K_{\text{a}2}$  (Figure 2b); (ii) the adsorption stoichiometry that best fits experimental data involves the reaction between one ligand anion, one  $\text{H}^+$ , and one neutral surface site (Figure 2b); (iii) as the oxide loading is increased, the height and the width of the plateau of maximum adsorption both increase (Figure 3B); (iv)  $\log K^{\text{S}}_{\text{intr}}$  determined from experiments with an oxide loading of 1 g/L can successfully predict adsorption behavior at loadings of 0.5 and 10 g/L (Figure 3B); (v) the experimentally measured extent of adsorption is unaffected by a change in ionic strength (Figure 4B); and (vi) the value of  $\log K^{\text{S}}_{\text{intr}}$  for substituted catechols increases with compound  $\text{p}K_{\text{a}}$  (Figure 6B).

Substituted catechols are easily susceptible to oxidation, and reliable adsorption data are difficult to obtain. For this reason, the adsorption behavior of only three substituted catechols was examined. As indicated in Figure 7, aromatic ring substituents influence the adsorption behavior of catechols. However, substituents have a smaller impact on catechol adsorption than on 2-aminophenol adsorption. 4-Nitro-2-aminophenol and 3-amino-2-naphthol, for example, adsorb significantly more strongly than does 4-chloro-2-aminophenol. When the analogous group of catechols is examined, the differences are less dramatic;

4-chlorocatechol adsorption is only slightly less than that of 4-nitrocatechol and 2,3-dihydroxynaphthalene.

Results of the modeling exercises of the adsorption behavior of catechols and 2-aminophenols differ in important respects. Experimentally measured adsorption of substituted 2-aminophenols and 3-amino-2-naphthol is best fit by a reaction stoichiometry that yields a surface complex with a neutral charge. In contrast, 4-nitrocatechol, 4-chlorocatechol, and 2,3-dihydroxynaphthalene adsorption is best fit through a reaction stoichiometry that yields a surface complex with a  $-1.0$  charge (eq 5, Table 2). The quality of the model fit at low ionic strength is also different for the two classes of compounds. In the case of 4-nitro-2-aminophenol, model predictions (using the stoichiometry and  $\log K_{\text{intr}}^{\text{s}}$  values from the high ionic strength experiments) match experimental data at low ionic strength. However, for 4-nitrocatechol, model predictions of adsorption at low ionic strength do not match experimental data; the model slightly overpredicts adsorption below pH 3.0, and dramatically underpredicts adsorption at high pH values (Figure 4B).

**Adsorption Behavior of 1,2-Phenylenediamines.** The extent of 4-nitro-1,2-phenylenediamine, 4-chloro-1,2-phenylenediamine, and 2,3-diaminonaphthalene adsorption was less than 5% in the pH range 2–11, even at  $\text{TiO}_2$  loadings as high as 15 g/L. For this reason, we were unable to determine  $\log K_{\text{intr}}^{\text{s}}$  values for these compounds. Ludwig and Schindler (14) found that the maximum extent of 1,2-phenylenediamine adsorption onto  $\text{TiO}_2$  (at comparable oxide loadings) was slightly higher than 5%, in agreement with our results.

## Discussion

Aminophenols and dihydroxybenzenes possessing Lewis base groups ortho to one another adsorb to a significant extent (e.g., 2-aminophenol and catechol) while those that possess Lewis base groups meta and para to one another do not (e.g., 3-aminophenol, 4-aminophenol, hydroquinone). Electronic effects are not responsible for these observations, since resonance interactions among ortho-substituted groups and among para-substituted groups are comparable. Instead, these observations provide indirect evidence that surface chelate formation takes place; Lewis base groups ortho to one another can simultaneously coordinate a single metal ion, while those meta or para to one another cannot. Similarly, cylindrical internal reflectance–Fourier transform infrared (CIR–FTIR) spectroscopy studies by Tunesi and Anderson (45) have shown that hydroxyl groups or amino groups substituted ortho to a carboxyl group (e.g., salicylic and anthranilic acids) may lead to a mononuclear bidentate coordination complex with a surface-bound Ti(IV) ion.

**Comparison between Aromatic Hydroxyl and Aromatic Amino Ligand Donor Groups.** As mentioned earlier, 4-nitro-2-aminophenol and 4-nitrocatechol adsorb more strongly onto  $\text{TiO}_2$  than the other substituted 2-aminophenols and catechols examined. For this reason, we have chosen to compare the adsorption behavior of the nitro-substituted ligands to understand the influence of ligand donor group identity. We observe that 4-nitrocatechol adsorbs more strongly than 4-nitro-2-aminophenol, while 4-nitro-1,2-phenylenediamine fails to adsorb. This trend can be interpreted in terms of what is currently known about the complex formation properties of Ti(IV) and the test ligands included in this study.

Complex formation results from both ionic and covalent contributions to bonding. The charge-to-radius ratio and the polarizability (the ease with which the electron distribution is distorted in an electrical field) of the elements involved in bond formation are the primary factors that dictate whether ionic or covalent contribution to bonding predominates. A high charge-to-radius ratio results in a high ionic contribution toward complex formation, while greater polarizability allows for a high covalent contribution toward complex formation (46).

Because of the high charge-to-radius ratio of Ti(IV), the ionic contribution toward bonding is predominant for all Ti(IV)–organic ligand complexes. A small covalent contribution to bonding (that compliments the ionic contribution) can also exist because the Ti(IV) lowest unoccupied molecular orbital, LUMO, (the empty  $d^0$  orbital) can accept electron density from the ligand. Thus, a covalent contribution can increase binding to Ti(IV)-containing surfaces, but only when the ionic contribution to bonding is already strong.

As far as Lewis base groups are concerned, the phenolate group possesses a negative charge and a high charge-to-radius ratio that yields a large ionic contribution to complex formation. The amino group, in contrast, possesses a neutral formal charge, and the ionic contribution to bonding is restricted to the interaction between ionic charge of the surface metal ion and the dipole moment of the amino group. Since ion–dipole interactions are known to be weak, the amino group has a lower contribution to ionic bonding. However, the greater polarizability of the lone pair electrons on nitrogen raises the covalent contribution to complex formation.

The ligands examined in this study possess pairs of ligand donor groups; their contributions to ionic and covalent bonding are likely to be cumulative. The presence of two hydroxyl donor groups (4-nitrocatechol) allows for the highest contribution to ionic bonding with the  $\text{TiO}_2$  surface, hence the greatest extent of adsorption. When one hydroxyl and one amino donor group are present (4-nitro-2-aminophenol), the contribution to ionic bonding is lower, resulting in a lower extent of adsorption. The ionic bonding contribution from two amino donor groups (4-nitro-1,2-phenylenediamine) is small, hence the extent of adsorption is negligible.

**Effect of Non-Ligand Ring Substituents.** We observe that a change in the identity of the ring substituent alters the extent of adsorption and the value of  $\log K_{\text{intr}}^{\text{s}}$  for both 2-aminophenols and catechols. The observed trends are explained by examining how variations in ligand properties resulting from ring substitution affect adsorption behavior. The presence of a substituent on an aromatic ring can change the properties of the organic ligand in a number of ways: (i) electronic effects alter the properties of ligand donor groups and (ii) changes in molecular size and dipole moment alter solvation energies (interactions between the ligand and surrounding water molecules).

**Electronic Effects.** It was established by Hammett (47) that the presence of a ring substituent can alter compound basicity (i.e., ability of the Lewis base groups to bind protons) via inductive and resonance electronic effects. Hammett (47) used differences in basicity ( $\text{p}K_{\text{a}}$ ) among benzoic acids as a means to explore the nature of the electronic effects of meta and para substituents. Based on these studies, substituent constants (referred to as Hammett constants,  $\sigma$ ) that measure the electron-withdrawing/electron-donat-

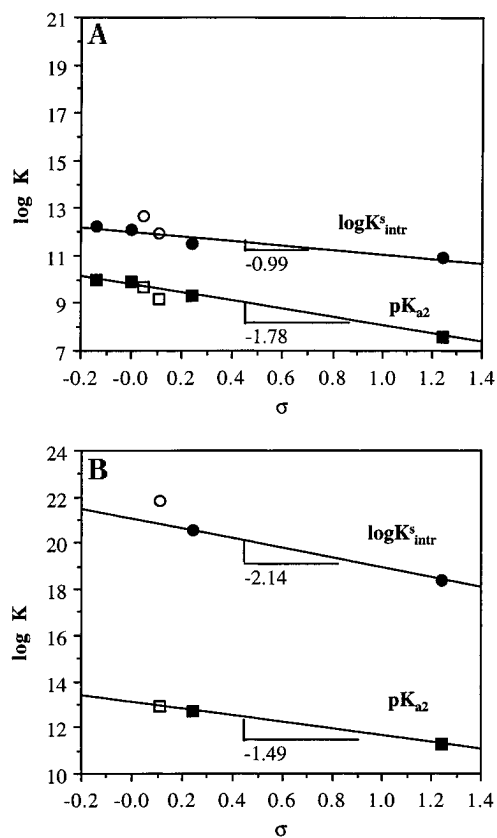


FIGURE 8.  $pK_{a2}$  and  $\log K^{\text{intr}}$  as a function of the Hammett Constant ( $\sigma_{\text{para}}$  or  $\sigma$ ) for (A) substituted 2-aminophenols and 3-amino-2-naphthol and (B) substituted catechols and 2,3-dihydroxybenzene. Compounds with an additional aromatic ring (open symbols) are omitted from the slope calculations.

ing capacity of aromatic ring substituents were determined. For several classes of compounds,  $pK_a$  was found to decrease with increasing  $\sigma$  (increasing electron-withdrawing capacity) (48).

Studies of metal–ligand complexation in solution have demonstrated that structurally related compounds with the same donor groups show a linear increase in the log of the equilibrium constant for metal complexation as the basicity ( $pK_a$ ) of the organic ligand is increased (or  $\sigma$  is decreased). A ligand that serves as an effective Lewis base toward protons also serves as an effective Lewis base toward metal ions (49–51). Figures 6 and 8 show that an analogous relationship may be valid for surface complexes:  $\log K^{\text{intr}}$  increases with increasing  $pK_a$  (and decreasing  $\sigma$ ) for both 2-aminophenols and catechols.

For both ligand classes (substituted 2-aminophenols and catechols), the nitro-substituted ligands adsorb to the greatest extent despite possessing the lowest values for  $pK_a$  and  $\log K^{\text{intr}}$ . Insight into this trend is gained by examining pertinent mass balance equations. For example, in the mass balance equation (eq 4) for 2-aminophenol, total

$$L_T = [H_2L^+] + [HL] + [L^-] + [>Ti-L] \quad (4)$$

ligand concentration ( $L_T$ ), dissolved ligand concentrations ( $[H_2L^+] + [HL] + [L^-]$ ), and adsorbed ligand concentrations ( $[>Ti-L]$ ) are all expressed in units of moles/liter of suspension. Rewriting this equation in terms of the lowest protonation level of the ligand yields

$$L_T = \{[H^+]^2/K_{a1}K_{a2} + [H^+]/K_{a1} + 1 + K^{\text{intr}}[H^+][>S]\}[L^-] \quad (5)$$

Thus, protons and surface sites compete for  $L^-$ ; the extent of adsorption depends upon the relative concentrations of protons and surface sites and upon the relative magnitudes of  $K_{a1}$ ,  $K_{a2}$ , and  $K^{\text{intr}}$ . For a change in the system to yield an increase in adsorption, the last term in eq 4 must grow at the expense of all preceding terms. An increase or decrease in adsorption, as a result of ring substitution, depends on changes in both  $pK_a$  values and  $\log K^{\text{intr}}$ .

The presence of an electron-donating or electron-withdrawing substituent affects  $pK_a$  values and  $\log K^{\text{intr}}$  values to different extents. Changes in  $pK_{a2}$  and  $\log K^{\text{intr}}$  as a function of  $\sigma$  can be compared to explore their relative sensitivity to electronic effects (Figure 8A–B). In this study, the substituent constant  $\sigma^-$  is used for the nitro substituent in order to account for through resonance with the phenolate group (52);  $\sigma_{\text{para}}$  values are used for all the remaining substituents.

Figure 8A indicates that both  $pK_{a2}$  and  $\log K^{\text{intr}}$  for substituted 2-aminophenols decrease with increasing  $\sigma$ ; the line depicting  $pK_{a2}$  as a function of  $\sigma$  has a slope equal to  $-1.78$ , while the line representing  $\log K^{\text{intr}}$  as a function of  $\sigma$  has a slope equal to  $-0.99$ . The difference in the slopes indicates that the affinity of the ligand for protons decreases more sharply than the affinity for the surface sites. This observation indicates that strongly electron-withdrawing groups such as the  $\text{NO}_2$  group depress proton binding more than surface site binding and, as a consequence, electron-withdrawing groups favor adsorption at the expense of protonation.

For catechols, the line depicting  $pK_{a2}$  as a function of  $\sigma$  has a slope equal to  $-1.49$ , while the line for  $\log K^{\text{intr}}$  has slope equal to  $-2.14$  (Figure 8B). It would be tempting at this point to conclude on the basis of the observed difference in slopes that the overall effect of electron-withdrawing substituents such as  $\text{NO}_2$  should be to decrease rather than to increase ligand adsorption. It must be kept in mind, however, that the intercept of the  $\log K^{\text{intr}}$  versus the  $\sigma$  line is considerably higher for catechols than for 2-aminophenols, yielding an across-the-board preference for adsorption over protonation.

**Solvation Effects.** Changes in solvation energy arising from the addition of a substituent are difficult to evaluate. The Henry's law constant (air to water distribution coefficient) is the best available measure of ligand solvation (53). However, few reliable values of Henry's law constants are available for compounds with multiple polar functional groups, such as those included in this study. In contrast, octanol–water partition coefficients ( $K_{ow}$ ) and aqueous solubilities ( $S_m$ ) are more frequently reported and can be more readily estimated (Table 1). Using such parameters as indicators of the degree of solvation (ligand–water interactions) must be done with caution: octanol–water partition coefficients include a measure of ligand–octanol interaction forces, and estimates of aqueous solubility include a measure of ligand–ligand interaction forces.

Compounds that possess two or more aromatic rings (e.g., 4-phenyl-2-aminophenol, 3-amino-2-naphthol, and 2,3-dihydroxynaphthalene) are more difficult to solvate than compounds with a single aromatic ring (54). This is substantiated by the fact that these ligands possess higher octanol–water partition coefficients and lower aqueous



solubilities (Table 1). The value of  $K_{ow}$  increases as the compounds become more hydrophobic, whereas the value of  $S_m$  decreases as the compounds become more hydrophobic. 4-Phenyl-2-aminophenol and 3-amino-2-naphthol adsorb to a greater extent than compounds with comparable  $pK_a$  values (Figure 5A–C) and have higher values for  $\log K_{intr}^s$  (Figure 6A). Similarly, 2,3-dihydroxynaphthalene adsorbs more strongly than the substituted catechol of comparable basicity, 4-chloro-catechol (Figure 7), and possesses a higher value of  $\log K_{intr}^s$  (Figure 6B). These observations can be attributed to the presence of an additional aromatic ring, which makes interaction with water less favorable. As a result, the ligand is excluded from bulk solution, and the extent of adsorption and, consequently, the value of  $\log K_{intr}^s$  are higher. This analysis establishes the importance of *both* basicity and hydrophobicity in determining the extent of adsorption and the value of  $\log K_{intr}^s$  for organic ligands with hydrophobic substituents.

Ring substituents have similar effects on the extent of adsorption of catechols and 2-aminophenols. However, the effect on catechol adsorption is less pronounced. It is likely that the high  $\log K_{intr}^s$  values obtained for catechols render this class of ligands somewhat less sensitive to substituent effects.

**pH Effects.** Adsorption is typically diminished at very high pH (where  $OH^-$  effectively competes with the deprotonated ligand for surface sites) and at low pH (where neutral surface sites are converted into protonated sites and ligand molecules become successively protonated) (Figure 3A,B). The pH affects the protonation equilibria of ligands in solution and the protonation level of individual surface sites. The net protonation level of the surface in turn determines surface charge and surface potential. Below the  $pH_{zpc}$  of the surface, positive surface charge increases with decreasing pH and above the  $pH_{zpc}$  negative surface charge increases with increasing pH.

**Ionic Strength Effects.** Ionic strength of the aqueous medium plays an important role in determining the long-range electrostatic forces and the near-range physical and chemical forces involved in ligand adsorption. An increase in ionic strength decreases the activity coefficient,  $\gamma$ , of the ions in solution (55). As a consequence, the relative concentration of protons and protonated and deprotonated forms of the ligand are altered. At high ionic strength, there is a greater density of electrolyte ions per fluid volume, the developing surface charge is easily balanced by counterions in the nearby solution, and the diffuse layer thickness is decreased. As a result, the surface potential ( $\psi_o$ ) is decreased, the surface is more easily charged, and long-range electrostatic interactions between dissolved ions and the charged surface are diminished (15). Additionally, if the adsorption of electrolyte ions (e.g.,  $Na^+$  and  $Cl^-$ ) is significant, ligand adsorption is expected to decrease at high ionic strength as the electrolyte ions are likely to compete with the ligand for available surface sites.

There are other subtle effects of ionic strength that are difficult to quantify. The concentration of electrolyte ions affects water–water, ligand–water, and surface–water interaction forces. Thus, solvation of the ligand in solution, the free surface sites, and surface–site–ligand complex are likely to be influenced by ionic strength.

In Figure 4, the diffuse layer model results are shown along with experimental adsorption data at 0.1 and  $10^{-3}$  M ionic strength. The diffuse layer model treats ions as point

charges and is believed to overestimate the degree of ion accumulation at charged surfaces at high ionic strength. In addition, the diffuse layer model does not have adjustable parameters that can explicitly account for all the factors that are sensitive to changes in ionic strength (e.g., solvation interactions and relative dielectric permittivity). In the diffuse layer model, parameter values (e.g.,  $K_{intr}^s$ ) determined at a given ionic strength are in principle “conditional constants” valid only for that ionic strength (31). For these reasons, successful prediction of adsorption at  $10^{-3}$  M ionic strength based on  $pK_a$  values and  $K_{intr}^s$  determined at 0.1 M ionic strength is not expected to occur.

However, it is interesting to note that the model extrapolation to  $10^{-3}$  M ionic strength is successful for 4-nitro-2-aminophenol. This is a consequence of adsorption stoichiometry (eq 2, Table 2) used to determine  $\log K_{intr}^s$ ; the long-range electrostatic correction terms for  $H^+$  and  $L^-$  exactly cancel out, yielding

$$K_{intr}^s = \frac{[>S-L^o]}{[>S][H^+]_b[L^-]_b} \quad (6)$$

The value of  $\log K_{intr}^s$  for 4-nitrocatechol adsorption, in contrast, was determined using an adsorption stoichiometry in which electrostatic correction terms for  $H^+$  and  $L^{2-}$  remain in the governing equation, yielding

$$K_{intr}^s = \frac{[>S-L^-]}{[>S][H^+]_b[L^{2-}]_b \exp(z_i F \psi_o / RT)} \quad (7)$$

As a consequence, model predictions based on eq 7 are more sensitive to changes in ionic strength than predictions based on eq 6. Therefore, for 4-nitrocatechol, either the choice of the adsorption stoichiometry or the procedure for estimating  $\psi_o$  is not accurate, causing the model to predict an ionic strength effect that is greater than the effect observed experimentally.

## Conclusions

By examining the adsorption behavior of three classes of organic ligands, we have been able to explore how hydroxyl and amino Lewis base groups and other aromatic ring substituents determine the extent of adsorption and the value of  $\log K_{intr}^s$ . In this work, physical–chemical phenomena that govern adsorption behavior were examined by making systematic changes to structure of the organic ligand and the composition of the aqueous medium. This approach could be profitably used to predict the adsorption behavior of other commercially important aromatic ligand compounds.

## Acknowledgments

Support by the Environmental Engineering Program of the National Science Foundation (Grant BES9317842) directed by Dr. Edward Bryan is gratefully acknowledged. We would like to thank Dr. Charles R. O’Melia, Dr. A. Lynn Roberts, and Dr. Gerald J. Meyer for their useful suggestions on the manuscript and Krassimir Bozhilov (Department of Earth and Planetary Sciences, Johns Hopkins University) for his help with the TEM and electron diffraction studies.

## Literature Cited

- McCarthy, J. F.; Zachara, J. M. *Environ. Sci. Technol.* **1989**, *23*, 496–502.

- (2) Biber, M. V.; Stumm, W. *Environ. Sci. Technol.* **1994**, *28*, 763–768.
- (3) Kung, K. S.; McBride, M. B. *Clays Clay Miner.* **1989**, *37*, 333–340.
- (4) Kung, K. S.; McBride, M. B. *Soil Sci. Soc. Am. J.* **1989**, *53*, 1673–1678.
- (5) Regazzoni, A. E.; Blesa, M. A.; Marotao, A. J. G. *J. Colloid Interface Sci.* **1988**, *122*, 315–325.
- (6) Balistrieri, L. S.; Murray, J. W. *Geochim. Cosmochim. Acta* **1987**, *51*, 1151–1160.
- (7) Chang, H. C.; Healy, T. W.; Matijevic, E. *J. Colloid Interface Sci.* **1983**, *92*, 469–478.
- (8) Kummert, R.; Stumm, W. *J. Colloid Interface Sci.* **1980**, *75*, 373–385.
- (9) Stumm, W.; Kummert, R.; Sigg, L. *Croat. Chem. Acta* **1980**, *53*, 291–312.
- (10) Rubio, J.; Matijevic, E. *J. Colloid Interface Sci.* **1979**, *68*, 408–421.
- (11) Davis, J. A.; Leckie, J. O. *Environ. Sci. Technol.* **1978**, *12*, 1309–1315.
- (12) Parfitt, R. L.; Farmer, V. C.; Russell, J. D. *J. Soil Sci.* **1977**, *28*, 29–39.
- (13) Parfitt, R. L.; Farmer, V. C.; Russell, J. D. *J. Soil Sci.* **1977**, *28*, 40–47.
- (14) Ludwig, L.; Schindler, P. W. *J. Colloid Interface Sci.* **1995**, *169*, 291–299.
- (15) Stone, A. T.; Torrents, A.; Smolen, J.; Vasudevan, D.; Hadley, J. *Environ. Sci. Technol.* **1993**, *27*, 895–909.
- (16) Hering, J. G.; Stumm, W. *Langmuir* **1991**, *7*, 1567–1570.
- (17) McBride, M. B.; Kung, K. H. *Environ. Toxicol. Chem.* **1991**, *10*, 441–448.
- (18) Zachara, J. M.; Ainsworth, C. C.; Cowan, C. E.; Schmidt, R. L. *Environ. Sci. Technol.* **1990**, *24*, 118–126.
- (19) McBride, M. B.; Wesselink, L. G. *Environ. Sci. Technol.* **1988**, *22*, 703–708.
- (20) Schellenberg, K.; Leuenberger, C.; Schwarzenbach, R. P. *Environ. Sci. Technol.* **1984**, *18*, 652–657.
- (21) Means, J. C.; Wood, S. G.; Hassett, J. J.; Banwart, W. L. *Environ. Sci. Technol.* **1982**, *16*, 93–97.
- (22) Schwarzenbach, R. P.; Westall, J. *Environ. Sci. Technol.* **1981**, *15*, 1360–1367.
- (23) Karickhoff, S. W.; Brown, D. S.; Scott, T. A. *Water Res.* **1979**, *13*, 241–248.
- (24) Tanford, C. *The Hydrophobic Effect*; Wiley-Interscience: New York, 1980.
- (25) Perlinger, J. A.; Eisenreich, S. J.; Capel, D. P. *Environ. Sci. Technol.* **1993**, *27*, 928–932.
- (26) Backus, D. Ph.D. Thesis, Massachusetts Institute of Technology, Cambridge, MA, 1990.
- (27) Stumm, W.; Morgan, J. M. *Aquatic Chemistry*; Wiley-Interscience: New York, 1981.
- (28) Herbelin, A.; Westall, J. C. *FITEQL 3*. Report 94-01; Department of Chemistry, Oregon State University: Corvallis, OR, 1994.
- (29) Papelis, C.; Hayes, K. F.; Leckie, J. O. *HYRAQL*. Technical Report 306; Department of Civil Engineering, Stanford University: Stanford, CA, 1988.
- (30) Westall, J. C.; Zachary, J.; Morel, F. M. M. *MINEQL*. Technical Note 18; Ralph M. Parsons Laboratory, MIT: Cambridge, MA, 1976.
- (31) Westall, J. C.; Hohl, H. *Adv. Colloid Interface Sci.* **1980**, *12*, 265–294.
- (32) Hochella, M. F. In *Mineral Water Interface Geochemistry*; Hochella, M. F., White, A. F., Eds.; Reviews in Mineralogy; Mineralogical Society of America: Washington, DC, 1990; Vol. 23.
- (33) Tejedor-Tejedor, M. I.; Anderson, M. A. *Langmuir* **1986**, *2*, 203–210.
- (34) Healy, T. W.; White, L. R. *Adv. Colloid Interface Sci.* **1978**, *9*, 303–345.
- (35) Ludwig, L.; Schindler, P. W. *J. Colloid Interface Sci.* **1995**, *169*, 284–290.
- (36) Hiemstra, T.; Van Riemsdijk, W. H.; Bolt, G. H. *J. Colloid Interface Sci.* **1987**, *133*, 91–104.
- (37) Hiemstra, T.; DeWit, J. C. M.; Van Riemsdijk, W. H. *J. Colloid Interface Sci.* **1987**, *133*, 105–117.
- (38) Barlin, G. B.; Perrin, D. D. *Q. Rev. Chem Soc.* **1966**, *20*, 75–101.
- (39) Clark, J.; Perrin, D. D. *Q. Rev. Chem Soc.* **1964**, *18*, 285–320.
- (40) *ClogP, Version 1*. Computer Program for predicting Octanol–Water Partition Coefficients; BioByte Corp.: Claremont, CA, 1994.
- (41) Yalkowsky, S. H.; Valvani, S. C. *J. Pharm. Sci.* **1980**, *69*, 912–922.
- (42) Sigg, L.; Stumm, W. *Colloids Surf.* **1981**, *2*, 101–117.
- (43) Torrents, A. Ph.D. Thesis, Johns Hopkins University, Baltimore, MD, 1992.
- (44) Berube, Y. G.; deBruyn, P. L. J. *J. Colloid Interface Sci.* **1968**, *28*, 92–105.
- (45) Perrin, D. D. *Organic Complexing Reagents*; Interscience Publishers: New York, 1964.
- (46) Tunesi, S.; Anderson, M. A. *Langmuir* **1992**, *8*, 487–495.
- (47) Hammett, L. P. *J. Am. Chem. Soc.* **1937**, *59*, 96.
- (48) March, J. *Advanced Organic Chemistry*; John Wiley and Sons Inc.: New York, 1985; p 244.
- (49) Chen, Y. T. *Co-ordination Chemistry-20*; Pergamon Press: New York, 1979; p 276.
- (50) Bjerrum, J. *Chem. Rev.* **1950**, *46*, 381–399.
- (51) Basolo, F.; Chen, Y. T. *J. Am. Chem. Soc.* **1954**, *76*, 956–959.
- (52) Lowry, T. H.; Richardson, K. S. *Mechanisms and Theory in Organic Chemistry*; Harper and Row Publishers: New York, 1987.
- (53) Wolfenden, R. *Science* **1983**, *222*, 1087–93.
- (54) Schwarzenbach, R. P.; Imboden, D. M.; Gschwend, P. M. *Environmental Organic Chemistry*; John Wiley & Sons, Inc: New York, 1993.
- (55) Castellan, G. W. *Physical Chemistry*; Benjamin/Cummings Publishing Co.: Reading: MA, 1983.
- (56) Martell, A. E.; Smith, R. M. *Critical Stability Constants*; Plenum: New York, 1982; Vol. 5.

Received for review August 17, 1995. Revised manuscript received December 6, 1995. Accepted December 12, 1995.<sup>⊗</sup>

ES950615+

<sup>⊗</sup> Abstract published in *Advance ACS Abstracts*, March 1, 1996.